

Nondiffracting beams for vortex tomography

J. Řeháček,¹ Z. Hradil,¹ Z. Bouchal,¹ A. B. Klimov,² I. Rigas,³ and L. L. Sánchez-Soto³

¹Department of Optics, Palacký University, 17. listopadu 12, 746 01 Olomouc, Czech Republic

²Departamento de Física, Universidad de Guadalajara, 44420 Guadalajara, Jalisco, Mexico

³Departamento de Óptica, Facultad de Física, Universidad Complutense, 28040 Madrid, Spain

We propose a reconstruction of vortex beams based on the implementation of quadratic transformations in the orbital angular momentum. The information is encoded in a superposition of Bessel-like nondiffracting beams. The measurement of the angular probability distribution at different positions allows for the reconstruction of the Wigner function.

© 2018 Optical Society of America

OCIS codes: 270.5585 Quantum information processing, 260.0260 Physical optics, 260.6042 Singular optics

In recent years, considerable attention has been paid to optical vortices; i.e., beams of light whose phase varies in a corkscrew-like manner along the direction of propagation. The vortex itself is a topological point defect in the wavefront that manifests as a null amplitude because the phase there is indeterminate [1, 2]. In addition, these beams carry orbital angular momentum (OAM) and have a topological charge ℓ that is specified by the total phase change $2\pi\ell$ along a contour around the vortex center.

Apart from their fundamental importance, vortex beams have found numerous applications [3]. Besides, entangled photons prepared in a superposition of states bearing a well-defined OAM provide access to multidimensional entanglement. This is of considerable importance in quantum information and cryptography [4, 5].

Determining the OAM state of a vortex requires knowledge of the phase distribution around the singularity. Since direct measurement of this phase in the visible is not possible, one needs to rely on interferometric techniques that work reasonably well both at the single-photon level [6] and for classical beams [7, 8].

The goal of this Letter is to bring forward a feasible *direct* reconstruction of an optical vortex. We recall that efficient methods of state reconstruction are of the greatest relevance. Since the first theoretical proposals, this discipline has witnessed a significant growth and laboratory demonstrations of state tomography span a broad range of systems [9, 10].

The canonically conjugate variable to OAM is the angle, so we shall need some basic concepts about this quantity. Through all this Letter we use a quantum notation, although the translation to a purely classical language is direct. Let us denote by L the OAM along the direction z of propagation. For our purposes, the simplest choice is to use the complex exponential of the angle $E = e^{-i\phi}$, which satisfies the commutation relation $[E, L] = E$ [11]. The action of E on the OAM eigenstates is $E|\ell\rangle = |\ell - 1\rangle$, and it possesses then a simple implementation by means of phase mask removing a charge +1 from a vortex state [12]. Since the integer ℓ runs from $-\infty$ to $+\infty$, E is a unitary operator whose eigenvectors $|\phi\rangle = \frac{1}{\sqrt{2\pi}} \sum_{\ell \in \mathbb{Z}} e^{-i\ell\phi} |\ell\rangle$ are states with a well-defined angle. A point particle is necessarily located at a single value of the periodic angular coordinate. However, for extended ob-

jects, such as fields, the eigenvalue ϕ might be not directly related to an angular position in the transverse plane, as we shall see.

This canonical pair describes the physics of a planar rotor. The phase space is then the discrete cylinder $\mathcal{S}_1 \times \mathbb{Z}$, where \mathcal{S}_1 is the unit circle (associated to the angle) and the integers \mathbb{Z} translate the discreteness of the OAM [13]. To properly represent a state described by the density matrix ϱ , we need to introduce a Wigner function. Following our approach in Ref. [14], we define the Wigner function for this pair as

$$W(\ell, \phi) = \frac{1}{2\pi} \int_{-\pi}^{\pi} d\phi' e^{i\ell\phi'} \langle \phi - \phi'/2 | \varrho | \phi + \phi'/2 \rangle, \quad (1)$$

whose analogy with the standard one for position and momentum is more than evident. It is advantageous to rewrite Eq. (1) as

$$W(\ell, \phi) = \frac{1}{2\pi} \sum_{\ell' \in \mathbb{Z}} \int_{-\pi}^{\pi} d\phi' e^{i(\ell'\phi - \ell\phi')} \varrho(\ell', \phi'), \quad (2)$$

where $\varrho(\ell', \phi')$ are the Fourier coefficients of $W(\ell, \phi)$, given by $\varrho(\ell, \phi) = e^{-i\ell\phi/2} \sum_{\ell'} e^{i\ell'\phi} \langle \ell' | \varrho | \ell' - \ell \rangle$. For $\ell = 0$ this is simply the Fourier transform of the OAM spectrum $\langle \ell | \varrho | \ell \rangle$.

As one step further, assume we are able to measure L^2 transformations on the input state followed by angular projections, that is,

$$\omega(\phi, \zeta) = \langle \phi | \exp(i\zeta L^2/2) \varrho \exp(-i\zeta L^2/2) | \phi \rangle. \quad (3)$$

Together with the OAM spectrum, these tomograms $\omega(\phi, \zeta)$ provide complete information. Indeed, one can check that

$$\varrho(\ell, \phi) = \frac{1}{2\pi} \int d\phi' e^{-i\ell\phi'} \omega(\phi', \phi/\ell), \quad (4)$$

so the measurement of $\omega(\phi, \ell)$ allows for the determination of $\varrho(\ell, \phi)$ and hence the full reconstruction of the Wigner function via Eq. (2).

The feasibility of this scheme relies on the implementation of the L^2 operation, which is precisely a free rotor. Our starting point is a monochromatic light beam whose complex scalar profile can be written in cylindrical coordinates

as $\Psi(r, \varphi, z) = \psi(r, \varphi, z) \exp(-ikz)$, where the envelope $\psi(r, \varphi, z)$ is a slowly varying function of z . In further consideration, we restrict ourselves to the paraxial regime and neglect polarization effects.

In the angle representation, L acts as $-i\partial_\varphi$ and the OAM eigenstates (which constitute an appropriate basis) are conveniently expressed (in the plane $z = 0$) by

$$\psi_\ell(r, \varphi) = \langle r, \varphi | \ell \rangle = A_\ell(r) \exp(i\ell\varphi), \quad (5)$$

where $A_\ell(r)$ is an arbitrary radial profile. Please, notice carefully that the polar angle φ in the transverse plane should not be confused with the rotor eigenstate ϕ . Next, we look at beams for which free propagation induces an L^2 transformation, as for them the tomography will be enormously facilitated. We thus require

$$\psi_\ell(r, \varphi, z) = e^{ial^2z} \psi_\ell(r, \varphi). \quad (6)$$

In this case the *free propagation* of the optical field corresponds to *free evolution* of the rotor. Since the free evolution of paraxial optical beams is determined by the wave equation $\Delta_\perp \psi_\ell - 2ik\partial_z \psi_\ell = 0$, where Δ_\perp is the transverse Laplacian, we obtain

$$r^2 \frac{d^2 A_\ell(r)}{dr^2} + r \frac{dA_\ell(r)}{dr} + (\ell^2 r^2 - 2ak\ell^2) A_\ell(r) = 0, \quad (7)$$

whose regular solution is given in terms of the Bessel function $A_\ell(r) \propto J_\ell(\sqrt{2ak}lr)$. Consequently, the beams we look for turn out to have an envelope

$$\psi_\ell(r, \varphi, z) = N_\ell J_\ell(\sqrt{2ak}lr) e^{ial^2z} e^{i\ell\varphi}. \quad (8)$$

As it happens with plane waves, these beams require infinite energy, so their practical generation relies in a spatial apodization of some kind. We take this into account in the normalization factor $N_\ell^2 = [2\pi \int_0^R dr r J_\ell(\sqrt{2ak}lr)]^{-1}$, R being the radius of this apodizing element.

Taking $a \sim 1$ guarantees that we are safely in the paraxial region $|a| \ll 2k/\ell^2$. In that case, the Bessel beams involved have central maxima of the size of a few millimeters and quadratic phases $al^2 \sim 10$ rad/m are induced in the free propagation. This confirms the feasibility of our proposal.

We can also understand the form of the vortices (8) in an alternative way. The paraxial free-space transfer function is $H(\rho, \theta) \propto \exp(-i\pi\lambda z\rho^2)$, where (ρ, θ) are polar coordinates in the spatial-frequency space and λ is the wavelength. Let us assume that all the nonvanishing frequency components of our field lie on a circle of radius ρ_0 , that is, $\hat{\psi}(\rho, \theta) \propto \hat{\psi}(\theta) \delta(\rho - \rho_0)$, where $\hat{\psi}(\rho, \theta) = \mathcal{F}[\psi(r, \varphi)]$ denotes the Fourier transform. Then, free propagation contributes just by an unessential overall phase factor, $\hat{\psi}'(\rho, \theta) = H(\rho, \theta) \hat{\psi}(\rho, \theta) = \exp(-i\pi\lambda z\rho_0^2) \hat{\psi}(\theta)$, so the transverse intensity distribution becomes independent of the distance z (and hence represents a nondiffracting beam). The particular case of the family (6) is obtained by taking $\rho_0 = \sqrt{2ak}|\ell|/(2\pi)$.

A general input state can be encoded into an optical beam by creating a superposition of these basis waves $\psi(r, \varphi) =$

$\sum_\ell c_\ell \psi_\ell(r, \varphi)$, which can be easily accomplished by an amplitude spatial light modulator displaying a hologram computed as an interference pattern of the required field $\psi(r, \varphi)$ and a reference plane wave.

After propagating a distance z the beam will evolve into a new superposition $\psi(r, \varphi, z) = \sum_\ell c_\ell e^{ial^2z} \psi_\ell(r, \varphi)$. But according to Eq. (3), this is just the required L^2 action with $\zeta = -az$. This is the main result of this paper: by choosing a particular form (8) of the OAM eigenstates, the highly nontrivial L^2 transformation is realized by a simple free beam propagation. This also provides an experimentally feasible optical realization of a free rotor.

After some simple calculations, the associated tomograms for the superposition field turns out to be

$$\omega(\phi, \zeta) = \frac{1}{2\pi} \left| \sum_{\ell \in \mathbb{Z}} c_\ell e^{i\ell\phi} e^{-i\zeta\ell^2/2} \right|^2. \quad (9)$$

By scanning the values of ζ , the beam can thus be reconstructed according to Eq. (4). This completes our proposed scheme. Naturally, (9) are independent of the rapid oscillating factor $\exp(-ikz)$.

As a last experimental detail, we need to assess the measurement of the angular spectrum in Eq. (3). For the field $\psi(r, \varphi)$ this reads as (taking for simplicity the plane $z = 0$)

$$\omega(\phi, 0) = P(\phi) = \left| \int d\varphi dr r \psi_\phi^*(r, \varphi) \psi(r, \varphi) \right|^2, \quad (10)$$

where $\psi_\phi(r, \varphi) = \langle r, \varphi | \phi \rangle$, and $|\phi\rangle$ is a field with well-defined angle. Note in passing that the angular spectrum $P(\phi)$ cannot be obtained, in general, by measuring the angular profile of the output beam, e.g., using a wedge-shaped aperture. In fact, as a consequence of the nontrivial radial profile of the OAM eigenstates, the states of $\psi_\phi(r, \varphi)$ are given by

$$\psi_\phi(r, \varphi) = \sum_{\ell \in \mathbb{Z}} e^{i\ell(\varphi - \phi)} J_\ell(\sqrt{2ak}lr). \quad (11)$$

Finally, using the cross-correlation theorem of Fourier analysis, one gets $P(\phi) = \left| \mathcal{F}^{-1}[\hat{\psi}_\phi(\rho, -\theta) \hat{\psi}(\rho, \theta)] \right|_{r=0}^2$. This result provides a simple interpretation of the tomographic setup. The angular states (11) are defined in such a way that by placing a transparency $\hat{\psi}_\phi(\rho, -\theta)$ in the Fourier plane, the unwrapping of azimuthal phase modulations occurs simultaneously for all the vortices in the superposition $\psi(r, \varphi)$. As a result, the on-axis interference observed at the output plane of the optical processor yields phase information about the coefficients c_ℓ . Different angular components can be readily accessed by rotating the filter transparency with respect to the optical axis.

The proposed experiment thus consists of the following four steps: (i) The input state is encoded into a superposition of Bessel-like beams $\psi_l(r, \varphi)$. (ii) This superposition is propagated a distance z . (iii) The angular distribution $\omega(\phi, z)$ is determined by measuring the intensity in the middle of the output plane of the optical processor as a function of the

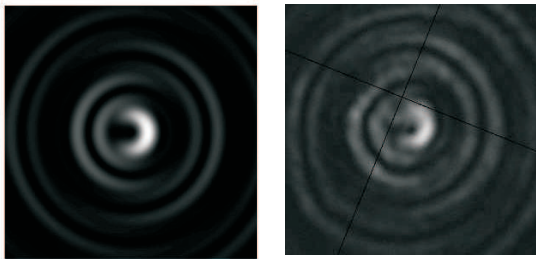


Fig. 1. (Color online) Calculated (left) and experimentally generated (right) transverse intensity distribution for a normalized superposition of the states $\psi_1(r, \phi)$ and $\psi_2(r, \phi)$.

Fourier filter orientation ϕ . The last two steps are repeated for a set of distances z . (iv) The Wigner function of the input state is reconstructed with the help of Eqs. (2) and (4).

As an illustration, we apply our reconstruction procedure to the state $\psi(r, \varphi) = [\psi_1(r, \varphi) + \psi_2(r, \varphi)]/\sqrt{2}$. The calculated transverse intensity of this state is shown in the left panel of Fig. 1, while a typical CCD scan of the state generated in the laboratory by an amplitude spatial light modulator (CRL Opto 1024×768 pixels) is shown on the right for comparison. As an illustration, we apply our reconstruction procedure to the state $\psi(r, \varphi) = [\psi_1(r, \varphi) + \psi_2(r, \varphi)]/\sqrt{2}$. The calculated transverse intensity of this state is shown in the left panel of Fig. 1, while a typical CCD scan of the state generated in the laboratory by an amplitude spatial light modulator (CRL Opto 1024×768 pixels) is shown on the right for comparison.

The tomograms are calculated from Eq. (9), whence we obtain the Fourier coefficients as $\varrho(\ell, \phi) = e^{i3\phi/2}(\delta_{\ell,1} + \delta_{\ell,-1})/(4\pi)$. This leads to the Wigner function

$$W(\ell, \phi) = \frac{1}{4\pi}(\delta_{\ell,1} + \delta_{\ell,2}) + \frac{(-1)^{\ell+1}}{\pi^2(3-2\ell)} \cos \phi. \quad (12)$$

We can see three contributions: two flat slices, coming from the fields ψ_1 and ψ_2 , located at $\ell = 1$ and $\ell = 2$, respectively,

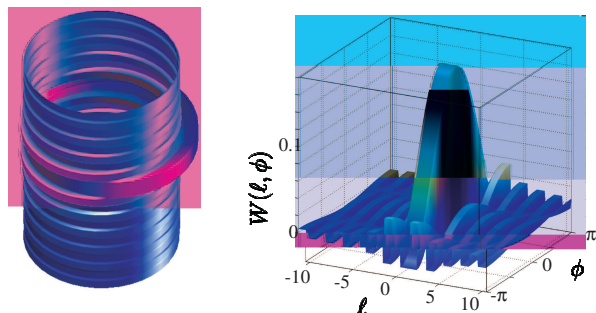


Fig. 2. (Color online) Reconstructed Wigner function (12) corresponding to the same state as in Fig. 1. Left panel shows this function on the unit cylinder (whose vertical axis corresponds to the OAM), while right panel show the unwrapped plot in Cartesian axis.

and an interference term that contains contributions from all the values of ℓ , although damped as $1/\ell$. These features are illustrated in Fig. 2, which shows the reconstructed Wigner function on the unit cylinder and its wrapped counterpart in Cartesian axes.

In practice, one cannot scan infinite values of ζ (i.e., of z), and only some discrete version of the Eq. (4) is available in the laboratory. We have checked that with 50 equispaced values, the reconstruction is still fairly stable.

In summary, we have carried out a full program for a complete reconstruction of vortex beams. In our scheme, the information is encoded in a superposition of Bessel-like non-diffracting beams for which free propagation is equivalent to the L^2 operation. At the same time, our formulation provides a theoretical framework on the action of angle and angular momentum on these beams.

References

1. M. Soskin and M. V. Vasnetsov, *Prog. Opt.* **41**, 219 (2001).
2. M. R. Dennis, K. O'Holleran, and M. J. Padgett, *Prog. Opt.* **53**, 293 (2009).
3. S. Franke-Arnold, L. Allen, and M. Padgett, *Laser Photon. Rev.* **2**, 299 (2008).
4. A. Mair, A. Vaziri, G. Weihs, and A. Zeilinger, *Nature* **412**, 313 (2001).
5. G. Molina-Terriza, A. Vaziri, J. Rehacek, Z. Hradil, and A. Zeilinger, *Phys. Rev. Lett.* **92**, 167903 (2004).
6. J. Leach, M. J. Padgett, S. M. Barnett, S. Franke-Arnold, and J. Courtial, *Phys. Rev. Lett.* **88**, 257901 (2002).
7. M. Harris, C. A. Hill, P. R. Tapster, and J. M. Vaughan, *Phys. Rev. A* **49**, 3119 (1994).
8. G. C. G. Berkhout and M. W. Beijersbergen, *Phys. Rev. Lett.* **101**, 100801 (2008).
9. M. G. A. Paris and J. Řeháček, eds., *Quantum State Estimation*, vol. 649 of *Lecture Notes in Physics* (Springer, Heidelberg, 2004).
10. A. I. Lvovsky and M. G. Raymer, *Rev. Mod. Phys.* **81**, 299 (2009).
11. J. Řeháček, Z. Bouchal, R. Čelechovský, Z. Hradil, and L. L. Sánchez-Soto, *Phys. Rev. A* **77**, 032110 (2008).
12. Z. Hradil, J. Řeháček, Z. Bouchal, R. Čelechovský, and L. L. Sánchez-Soto, *Phys. Rev. Lett.* **97**, 243601 (2006).
13. M. Asorey, P. Facchi, V. I. Man'ko, G. Marmo, S. Pascazio, and E. G. C. Sudarshan, *Phys. Rev. A* **76**, 012117 (2007).
14. I. Rigas, L. L. Sánchez-Soto, A. B. Klimov, J. Řeháček, and Z. Hradil, *Phys. Rev. A* **78**, 060101 (R) (2008).